

## Results on the 1 MW CW 170 GHz gyrotron TH1509UA for ITER and DTT at the FALCON test stand

Falk Braumueller<sup>1\*</sup>, Timothy P. Goodman<sup>1</sup>, Jérémy Genoud<sup>1</sup>, Ferran Albajar<sup>2</sup>, Stefano Alberti<sup>1</sup>, Konstantinos A. Avramidis<sup>3</sup>, Ruggero Bertazzoni<sup>2</sup>, William Bin<sup>4</sup>, Daniele Bonetti<sup>5</sup>, Alessandro Bruschi<sup>4</sup>, Antonio Cammi<sup>6</sup>, Mario Cavinato<sup>2</sup>, Ioannis Chelis<sup>3</sup>, Davide Dall'Acqua<sup>2</sup>, Rosa Difonzo<sup>7</sup>, Lukas Feuerstein<sup>8</sup>, Eleonora Gajetti<sup>7</sup>, Gerd Gantenbein<sup>8</sup>, Saul Garavaglia<sup>4</sup>, Jérémy Gontard<sup>9</sup>, Gustavo Granucci<sup>4,11</sup>, Jean-Philippe Hogge<sup>1</sup>, Stefan Illy<sup>8</sup>, Carolina Introini<sup>6</sup>, Zisis Ioannidis<sup>12</sup>, John Jelonnek<sup>8</sup>, Jianbo Jin<sup>8</sup>, Alberto Leggieri<sup>9</sup>, François Legrand<sup>9</sup>, Christophe Lievin<sup>9</sup>, Rodolphe Marchesin<sup>9</sup>, Ijaze M. Oumar<sup>9</sup>, Oriol Picas<sup>2</sup>, Afra Romano<sup>10,11</sup>, Tomasz Rzesnicki<sup>8</sup>, Francisco Sanchez<sup>2</sup>, Laura Savoldi<sup>7</sup>, Sebastian Stanculovic<sup>8</sup>, Ioannis Tigelis<sup>3</sup>, Etienne Vallée<sup>9</sup>, and Manfred Thumm<sup>8</sup>

<sup>1</sup>Swiss Plasma Center (SPC), Ecole Polytechnique Fédérale de Lausanne, CH-1015 Lausanne, Switzerland

<sup>2</sup>European Joint Undertaking for ITER and the Development of Fusion Energy (F4E), Barcelona, E-08019, Spain

<sup>3</sup>Department of Physics, National and Kapodistrian University of Athens (NKUA), University Campus, 15784, Athens, Greece

<sup>4</sup>Istituto per la Scienza e la Tecnologia dei Plasmi, Consiglio Nazionale delle Ricerche, 20125 Milano, Italy

<sup>5</sup>EniProgetti, 30175 Venezia Marghera, Italy

<sup>6</sup>Department of Energy, Polytechnic of Milano, 20133 Milano, Italy

<sup>7</sup>Department of Energy "Galileo Ferraris" (DENERG), Polytechnic of Turin, 10129 Torino, Italy

<sup>8</sup>Institute for Pulsed Power and Microwave Technology, Karlsruhe Institute of Technology (KIT), 76131 Karlsruhe, Germany

<sup>9</sup>Microwave Imaging Sub-Systems, THALES, Vélizy-Villacoublay, France, F-78141

<sup>10</sup>ENEA, Fusion and Nuclear Safety Department, C. R. Frascati, 00044 Frascati, Italy

<sup>11</sup>DTT S.C. a r.l., 00044 Frascati, Italy

<sup>12</sup>Department of Aerospace Science and Technology, National and Kapodistrian University of Athens, 34400 Psachna, Greece

**Abstract.** In this contribution, the tests of the pre-series gyrotron TH1509UA for the Divertor Tokamak Test facility (DTT) at the FALCON test facility are presented. This versatile test bed proves useful for testing continuous wave (CW) high-power gyrotrons, but also serves as a platform for testing components for the transmission line or the Upper Launcher of ITER and DTT. The gyrotron has demonstrated a power level of 1.02 MW at the gyrotron output window, corresponding to 980 kW at the output of the Matching Optics Unit (MOU) with a power variation during the pulse of < 2% after a stabilisation period. Additionally, an efficiency of 40% has been demonstrated during five consecutive 100 s pulses. Compared to the previous version, TH1509U, this gyrotron demonstrates the successful prevention of parasitic mode excitation over a wide range of parameters around the design operating point. The potential for even higher power performance has been shown in short pulses but not explored in long pulses yet, which instead focused on demonstrating compliance with the required specifications for the DTT project.

### 1 Introduction

The first THALES preseries gyrotron TH1509UA for the Divertor Tokamak Test facility (DTT) is currently being tested at the FALCON test stand established by Fusion for Energy and hosted by the Swiss Plasma Center (SPC) of the EPFL. DTT is under construction in Frascati, Italy, and the DTT plasma heating will rely for Electron Cyclotron Resonance Heating (ECRH) in the first stage on 16 gyrotrons [1] of this type from THALES, with the same design as the one of the European gyrotron for ITER.

The ECRH for ITER will be provided by 24 gyrotrons in the first stage. In order to design and develop the European contribution to the ITER ECRH sources, consisting in 6 gyrotrons in the first stage, the European Gyrotron Consortium (EGYC) was formed. EGYC is cur-

rently composed of the following institutions: the Ecole Polytechnique Fédérale de Lausanne (SPC-EPFL) in Lausanne, Switzerland, the Karlsruhe Institute of Technology in Germany (KIT), the National and Kapodistrian University of Athens in Greece (NKUA) and the National Research Council in Italy (ISTP-CNR). The collaboration is completed by the Polytechnic of Torino (PoliTO) and the Polytechnic of Milano (PoliMI, Italy) for contributions to the cooling circuit development and cathode heating control, respectively. EGYC works in close collaboration with the industrial partner THALES, who is responsible for the industrial design and manufacturing.

The design of the TH1509UA gyrotron is based on the design of the gyrotron TH1507 for the Stellarator Wendelstein 7-X [2], which led to the development of a 1 MW gyrotron for ITER. The design of the EU 1 MW / 170GHz

\*e-mail: falk.braunmuller@epfl.ch

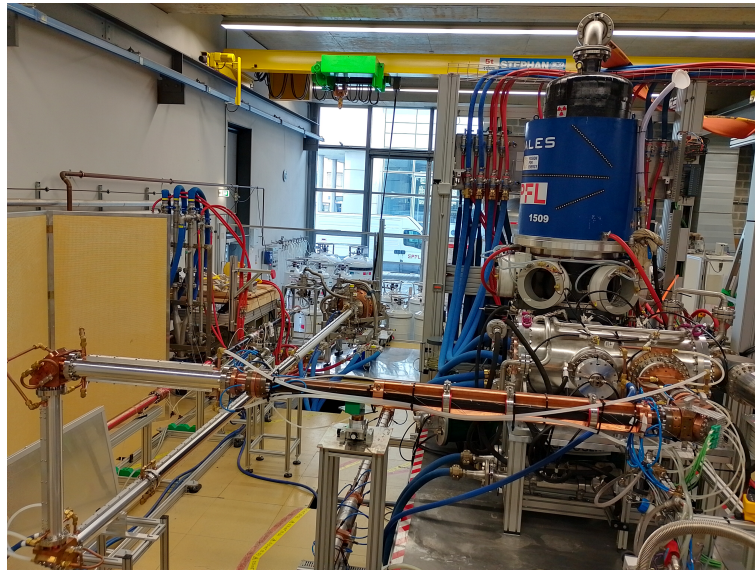


**Figure 1.** Gyrotron TH1509UA in the FALCON test facility.

gyrotron is based on a diode Magnetron Injection Gun (MIG), a super-conducting magnet operated at a cavity field of  $B_{cav} = 6.7$  T and a single-stage depressed collector.

During the continuous development from the TH1509 towards the TH1509UA [3, 4], minor design modifications have been integrated in several steps since the first prototype [5], in the beam tunnel, the high-voltage feedthroughs and insulation, the cathode structure and the cavity in order to pursue the industrialisation, optimise the power output and prevent the excitation of parasitic oscillations.

With these modifications, the gyrotron TH1509U for ITER successfully passed the qualification criteria for the ITER project [6] by demonstrating 0.95 MW over 100 seconds. Additionally, it demonstrated the ITER-required pulse length of 1000 seconds pulse with a power of 0.82 MW and an efficiency of 40%. However, this performance was limited by the appearance of parasitic oscillations in long pulses. Therefore, the current model includes further modifications to avoid the excitation of parasitic oscillations.

The design of the TH1509UA was first validated with a short-pulse modular gyrotron prototype at KIT, during which the beam radius was varied between  $R_b = 9.35$  mm and 9.65 mm and the velocity pitch factor  $\alpha = 1.0 - 1.6$  and the gyrotron was tested beyond the nominal operating parameters up to a beam current of  $I_b < 66$  A, resulting in a maximum power of 1.6 MW and 33% efficiency without depressed collector. In contrast to the previous version, this was demonstrated without excitation of parasitic oscillation [7].

Figure 1 shows the TH1509UA gyrotron in the present current configuration at the FALCON test facility with the final version of the Matching Optics Unit (MOU) at the gyrotron, followed by a 10 m transmission line (TL) connected to a calorimetric RF load which was initially developed by CNR and manufactured by CURTI Costruzioni Meccaniche SpA. The transmission line and RF-load were

supplied by US-ITER.

In the following section 2, first the setup and role of FALCON will be explained, followed by section 3 describing the current test results of the gyrotron, and finally section 4 presents the conclusions and outlook.

## 2 The FALCON test facility

The FALCON test facility is a European Technology Hub hosted by SPC at EPFL, mostly funded by F4E, with the purpose of testing both ECRH components and gyrotrons for ITER and other experimental devices [8]. It includes two gyrotron test stands, one hosting the TH1509UA gyrotron and the other hosting a ITER-type gyrotron manufactured by GYCOM. The two test beds are fed by the same high-voltage power supply and a cooling system which were dimensioned for an operation at 2 MW continuous output power at min. 40% efficiency. The current data acquisition and control system is supplied by F4E, in line with the one that is being developed for ITER.

Thanks to the strong collaboration between SPC, F4E, THALES, US ITER and DTT, all parties benefit from extended testing within the FALCON test bed. In general, transmission line components can be used for gyrotron testing and vice versa.

Since the creation of the FALCON test facility, the test bed has been used for gyrotron testing and commissioning in order to test different configurations of the EU 170 GHz / 1 MW prototype and the DTT pre-series gyrotron.

At the same time, FALCON has played a major role for testing ECRH components, namely components of both the ITER ECRH transmission line supplied by US ITER and of the ITER ECRH Upper Launcher developed by F4E. The tested components include evacuated corrugated waveguides, three different matched 170 GHz / 1 MW RF loads, a transmission line switch for switching between different waveguide outputs, a DC break, a pumpout unit,

expansion units, an MOU-adaptor and miter bends (including one with embedded thermocouples) at 90° and at 140° angle, which all have been tested with Megawatt-level power long RF pulses (tens of seconds) [8–11].

The future planning at FALCON consists in first the completion of the TH1509UA acceptance tests, after which the gyrotron will remain at FALCON in order to support further component testing. Beside the test of transmission line and ex-vessel waveguide components for US ITER, F4E and DTT, the planned component tests include a stray radiation test for the ITER Upper Launcher. A full-size thin-walled, unevacuated mock-up of the ITER Upper Launcher will be tested for stray radiation distribution by transmitting a pulse train of short (~1 s) Megawatt-level pulses through each of the input transmission lines, in sequence. The stray radiation will be measured using infrared cameras as well as bolometers and will be compared to calculations of the simulated total stray radiation [12].

### 3 Long-pulse test results of the TH1509UA gyrotron

At FALCON, the DTT pre-series gyrotron TH1509UA is currently undergoing long-pulse tests for commissioning. While the short-pulse tests at KIT included, amongst other things, a maximisation of the output power, the current tests at FALCON are only focused on demonstrating the operating parameters specified for DTT. Thus, the pulse length was limited to 100 seconds according to the DTT specifications. As reported in [13], the gyrotron successfully passed the pre-acceptance test with 100 seconds pulses. These tests were performed with a non-final setup using the MOU and super-conducting magnet which were available at FALCON. As an acceptance criteria, the gyrotron achieved five consecutive pulses with an average of 1.02 MW at the window and with a gyrotron efficiency of 40%. The inter-pulse standard deviation of 0.01 MW between the pulses illustrates the pulse-to-pulse repeatability.

Thus, while the previous gyrotron's power was limited by parasitic oscillations to 0.95 MW over 100 seconds at an efficiency of 35% (or 0.82 MW / 1000 s), the current gyrotron reached the Megawatt threshold with no detection of parasitic oscillations over a large range of operating parameters. The improved performance is illustrated by the increase of efficiency to 40% without being fully optimized. With respect to ITER specifications, it is foreseen that operation at 1MW / 1000 s can be achieved without any obstacle as successful long pulses showed stable operation, and further optimisation will be necessary in order to comply with the ITER requirement of 50% efficiency.

The operating point for these pulses was a cavity magnetic field of  $B_{cav} = 6.69$  T, an accelerating voltage of  $V_{acc} = 79.5$  kV with a depressed collector voltage of  $V_{body} = 24.5$  kV, an average beam current of  $I_{beam} = 48$  A, an electron guiding center radius of  $R_g = 9.55$  mm in the cavity and an electron velocity pitch factor of  $\alpha = 1.29$  (from simulations with ARIADNE [14]).

The power is obtained by a calorimetric measurement using the cooling flows and temperature differences from

the matched millimeter wave load, the transmission line and the MOU. The power measurement of the FALCON test stand has been confirmed by comparing three different 170 GHz loads. As an example, the time evolution of the measured power is shown in Fig. 2 for the last of these pulses, showing the calorimetric measurements of different components of the gyrotron as well as transmission line and load. One observes that towards the end of the 100 second pulse all components except the MOU approach a temperature equilibrium. The long time constant of the calorimetric measurement is due to a non-instantaneous heat dissipation and due to water transit times up to the point of temperature measurement.

The pulse-averaged powers of the 100 s pulse shown in

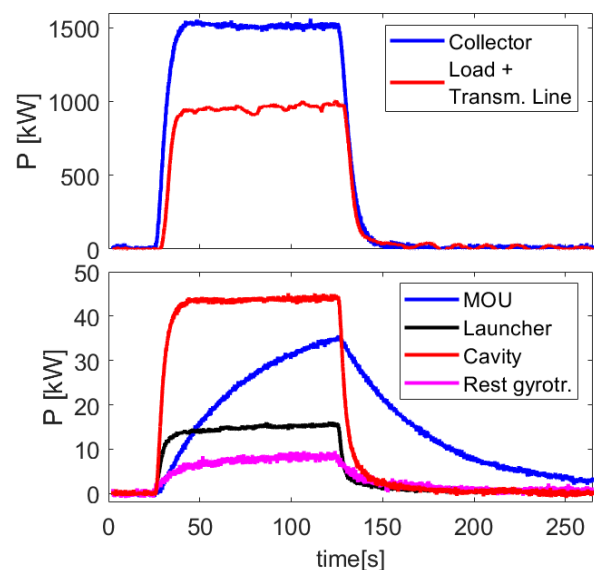


**Figure 2.** Evolution of the power measurement for the load and transmission line, the MOU and different parts of the gyrotron. The pink line in the lower plot ("Rest gyrotr.") corresponds to the sum of the power absorbed in several gyrotron sub-components such as a mirror and the relief load.

table 1 are calculated by integrating the energy of the entire pulse. The losses in the two-miter-bend transmission line were measured to be 2.4%, but in the experiments presented here they are measured together with the load calorimetry. In the five pulses of the pre-acceptance test, the power of the pulse-integrated calorimetry corresponds to the input electrical power to within 0.2-3%.

Fig. 3 shows the frequency temporal evolution within a 100 s pulse. In order to illustrate the initial frequency shift, the small insertion shows a zoom into the first second of a gyrotron pulse on a similar operating point. On the figure, the spectrogram of the measured frequency is shown, using 250 short acquisitions of 1μs (every 400 ms), of the frequency, which is down-converted via a heterodyne mixer and recorded with a sampling rate of 40 GS/s. The average frequency is 169.946 GHz for the 1.03 MW pulse. As shown in the zoomed insert from a similar pulse, the gyrotron frequency decreases over the first 0.5 seconds due to the thermal expansion of the cavity heated by the ohmic losses in the cavity wall. Thus, the output frequency is

**Table 1.** Calorimetric power balance over 100 s gyrotron pulse, calculated by integrating the energy over the pulse. Mir1 - Mir2 are the gyrotron internal mirrors. "Rest gyrotron" corresponds to the sum of the power absorbed in several gyrotron sub-components such as a mirror and the relief load.

Power type	Measurment.	Percentage
Electrical input:	2596.2 kW	100.00%
Collector:	1550.2 kW	59.71%
Load+Preload+TL:	990.4 kW	38.15%
MOU:	42.1 kW	1.62%
Cavity+Beam Tunnel+Mir1:	45.3 kW	1.74%
Launcher+Mir1+Mir2:	16.4 kW	0.63%
Rest gyrotron:	9.9 kW	0.39%
Total Cooling Circuits:	2654.3 kW	102.24%

directly linked to the gyrotron power, and frequency variations can be interpreted as power variations. In the present case, the measured dependency using a fit of experimental data over many pulses is  $\Delta P$  [kW]  $\propto 3.0 \cdot \Delta f$  [MHz]. For the time interval 20 - 100 s the maximum deviation of the measured frequency is only +/- 6 MHz. Although this variation may as well be linked to voltage variations, we can conclude from the maximum frequency variation that the variation in power is  $\leq \pm 20$  kW or  $< 2\%$ .

The observed change in frequency between 2 and 20 sec-

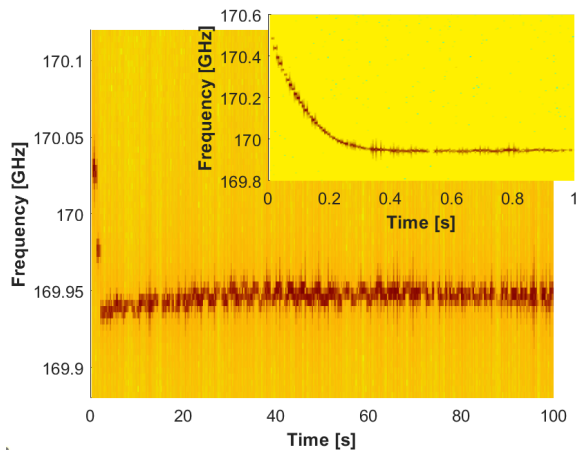


**Figure 3.** Spectrogram showing the instantaneous gyrotron frequency during 100 s long gyrotron pulse. The variation of the measured spectral maximum in frequency is of max. +/- 6 MHz after a stabilisation time of 20 seconds.

onds is caused by the variation of the beam current emitted from the cathode. Due to the thermionic emission cooling effect, the cathode temperature is reduced by the emitted electrons carrying away thermal energy from the cathode when emitting the beam current. The lower cathode temperature reduces the beam current. In order to reduce this effect, both the acceleration voltage and the filament heating current are changed in two predefined steps. As shown in figure 4, this scheme of current stabilisation limits the drop in beam current to 8 A. The current scheme includes an increase in voltage in two steps in the first 2 seconds, combined with an increase of the cathode heating filament

current in order to stabilize the beam current. The current stabilisation is being further improved and a feedback current controller is being developed in order to further minimise the beam current variation during long-pulse operation.

Around the operating point illustrated above, the gyrotron

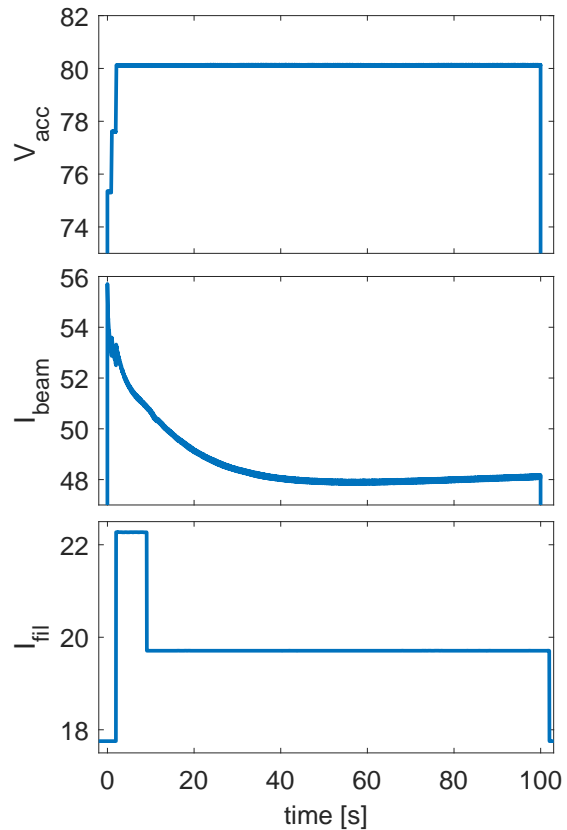


**Figure 4.** Beam current evolution and feed-forward control of the beam current in the initial phase of gyrotron pulse. The acceleration voltage is increased in two steps and the cathode filament heating current is varied in two steps as well.

operates in the design transverse mode without the presence of parasitic modes in a wide range of parameters. This is illustrated in Figure 5, which shows the power at the gyrotron window for a scan over the accelerating voltage ( $V_{cathode} + V_{body}$ ), measured using 30 s pulses. As can be seen, the power is more than doubled over a range of 6.5 kV.

During this scan, the gyrotron body voltage was increased from  $V_{body} = 20$  to 26 kV, the beam current increases from  $I_{beam} = 40$  to 46 A and the velocity pitch angle changes from  $\alpha = 1.13$  to 1.27. As the current is lower compared to the 100 second pulses shown above, the maximum power of the voltage scan does not reach 1 MW. Because the varied body voltage corresponds to the depression potential, the efficiency strongly varies during this scan, from 22 to 40%.

In order to couple the maximum power into the transmission line, the gyrotron has been designed for maximizing

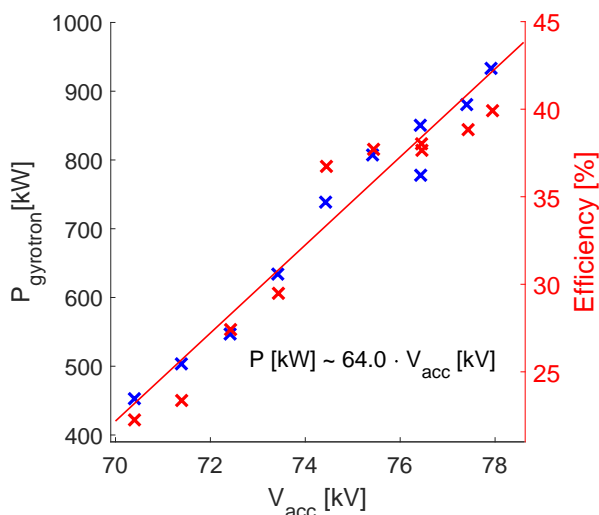


**Figure 5.** Gyrotron power at the window (in blue) and efficiency (in red) as a function of the accelerating voltage ( $V_{cathode} + V_{body}$ ) for an operating point of  $B_{cav} = 6.69$  T,  $V_{cathode} = 51 - 52.5$  kV,  $V_{body} = 20 - 26$  kV,  $I_{beam} = 40 - 46$  A,  $\alpha = 1.29$

the coupling to the  $HE_{11}$  waveguide mode. The gyrotron output beam pattern at the window is shown in Fig. 6. This beam pattern has been obtained by an iterative phase reconstruction method [15] from infrared measurements at several distances and subsequent propagation of the complex field pattern onto the plane of the window. It can be seen that the beam pattern is highly Gaussian and with a close to flat phase profile over a wide area. According to this measurement, the beam exits the gyrotron window with a small offset of 7 mm to the lower left of the center of the window, combined with a small angle of  $0.6^\circ$  to the lower left. The measured waist in horizontal and vertical direction is  $w_{0x} = 21.1$  mm /  $w_{0y} = 20.8$  mm, compared to the waist obtained from simulations which is  $w_{0x} = 19.4$  mm /  $w_{0y} = 19.6$  mm. The MOU allows for an optimized coupling of this beam into the waveguide and transmission line. The calculated maximum coupling efficiency of this output beam via the MOU into the  $HE_{11}$  mode of the 50 mm corrugated waveguide is 95.4 - >96%.

In the experiments presented here, two different versions of the MOU have been used. The first version includes 5 mirrors and corresponds to a MOU which has been repurposed from the EU 2 MW coaxial gyrotron project. It has been pre-aligned according to the measured gyrotron beam pattern with the help of a low-power microwave source at 170 GHz. With only the pre-alignment and no adjustment of the mirrors at high power, the measured losses in MOU and transmission line were close to those obtained from the classical alignment method - mirror by mirror while using burn-patterns on the MOU mirrors. The calorimetrically-measured losses in the first version of the MOU amount to approximately 4.2%. The second, recently installed MOU has been specially designed for DTT and ITER purposes, i.e. without polarizability requirements, and uses only two curved mirrors. In this

MOU, seen in Fig.1, the measured losses were approximately 2.2% in a preliminary alignment.

## 4 Conclusion and Outlook

For the first time, the EU 170 GHz gyrotron manufactured by THALES has reached the threshold of 1 Megawatt for 100 second pulses at the FALCON test facility. In the pre-acceptance tests a power of 1.02 MW was achieved and an efficiency of 40% without a full optimisation of the efficiency. The gyrotron shows stable and repeatable operation over a wide range of parameters without being limited by parasitic oscillations.

For these 100 s pulses, it is deduced from the frequency variations that the power varies by less than 2% for the last 80 seconds of the pulse. This is supported by a feed-forward current stabilisation, which is being further improved. The tests of the TH1509UA gyrotron are still ongoing and its performance is expected to be further enhanced. As a next step, the acceptance tests of the DTT pre-series gyrotron will continue in a modified configuration with its final MOU and super-conducting magnet. At the same time the tube's performance will be further optimised, such as its efficiency. Its final acceptance is planned for summer 2024.

In addition to the tests of the DTT pre-series gyrotron, FALCON is proving its versatility for high-power component testing especially for components of the ITER transmission line, ex-vessel waveguide and ECRH Upper Launcher.

## 5 Acknowledgements

This work is partially supported by Fusion for Energy under Task Order 5 of the Framework contract F4E-OFC-0671. The views expressed in this publication are the sole responsibility of authors and do not necessarily reflect the views of F4E, European Commission or ITER Organization.

The authors warmly thank Greg Hanson for the use of US ITER test equipment during the described tests.

## References

- [1] S. Garavaglia et al., "Progress of DTT ECRH system de-sign", en, [Fusion Engineering and Design](#) **168**, 112678 (2021).
- [2] M. Thumm et al., "EU Megawatt-Class 140-GHz CW Gyrotron", en, [IEEE Transactions on Plasma Science](#) **35**, 143–153 (2007).
- [3] I. G. Pagonakis et al., "Status of the development of the EU 170 GHz/1 MW/CW gyrotron", en, [Fusion Engineering and Design](#) **96-97**, 149–154 (2015).
- [4] Z. C. Ioannidis et al., "Recent experiments with the European 1MW, 170GHz industrial CW and short-pulse gyrotrons for ITER", en, [Fusion Engineering and Design](#) **146**, 349–352 (2019).

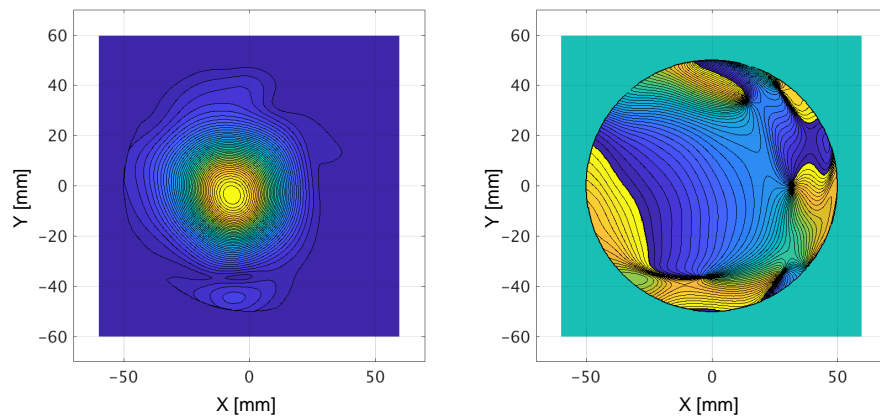


**Figure 6.** Reconstructed amplitude and phase pattern of the beam on the gyrotron window. The beam is reconstructed using the beam pattern measured by a thermal imaging of short pulses at different distances from the window.

- [5] A. Leggieri et al., “TH1509U European 170 GHz 1 MW CW Industrial Gyrotron Upgrade”, en, in [2021 22nd International Vacuum Electronics Conference \(IVEC\)](#)(Apr. 2021), pp. 1–2.
- [6] T.P. Goodman et al., “Tests and Qualification of the European 1 MW, 170 GHz CW Gyrotron in an ITER relevant configuration at SPC”, en, in [2022 47th International Conference on Infrared, Millimeter and Terahertz Waves \(IRMMW-THz\)](#) (Aug. 2022), pp. 1–2.
- [7] T. Rzesnicki et al., “Parasitic-modes free, high-performance operation of the European 1 MW, 170 GHz Short-Pulse Prototype Gyrotron for ITER”, en, in [2023 48th International Conference on Infrared, Millimeter, and Terahertz Waves \(IRMMW-THz\)](#) (Sept. 2023), pp. 1–2.
- [8] T. P. Goodman et al., “High-Power Testing of Guided-Wave Components for the ITER ECH Upper Launcher at the FALCON Test Facility”, en, [IEEE Transactions on Plasma Science](#) **48**, 1537–1542 (2020).
- [9] G. Hanson et al., “ITER ECH Transmission Line System Design and Status”, in [22nd Joint Workshop on Electron Cyclotron Emission \(ECE\) and Electron Cyclotron Res-onance Heating \(ECRH\)](#) (Apr. 2024).
- [10] A. Xydou et al., “Prototype mitre bends of the ex-vessel waveguide system for the ITER upper launcher: Thermal hydraulic simulations and experiments with off-center mm-wave beams”, en, [Fusion Engineering and Design](#) **170**, 112457 (2021).
- [11] T. P. Goodman et al., “High power mm-wave loss measurements of ITER ex-vessel waveguide components at the FALCON test facility at the Swiss Plasma Center”, en, [EPJ Web of Conferences](#) **277**, 04010 (2023).
- [12] A. Avilés et al., “Integrated RF Analysis of the beam propagation and stray radiation in the ITER ECRH Upper Launcher”, in [33rd Symposium on Fusion Technology](#) (Sept. 2024).
- [13] A. Leggieri et al., “Industrial Qualification of the THALES TH1509U European 170 GHz 1 MW CW Gyrotron”, in [25th International Vacuum Electronics Conference \(IVEC\)](#) (2024).
- [14] J. Pagonakis and J. Vomvoridis, “The self-consistent 3D trajectory electrostatic code ARIADNE for gyrotron beam tunnel simulation”, en, in [Infrared and Millimeter Waves, Conference Digest of the 2004 Joint 29th International Conference on 2004 and 12th International Conference on Terahertz Electronics, 2004.](#) (2004), pp. 657–658.
- [15] S. K. Jawla, “Phase Retrieval and Gaussian Beam Mode Decomposition of Gyrotron Beams”, PhD thesis (EPFL, 2010).